Supporting Information

Electrocatalytic NO reduction to NH_3 over TiS_2 nanosheets

Xiangli Wang [1*], Lan Yang [1], Guike Zhang [2], Ke Chu [2]

[1] *College of Electrical Engineering, Northwest MinZu University, Lanzhou 730030, China*

[2] *School of Materials Science and Engineering, Lanzhou Jiaotong University, Lanzhou 730070, China*

*Corresponding author. wxl2002wxl@163.com (X.L. Wang)

Experimental Section

Materials

TiS_2 powder (≥99.9 wt%), C_3H_8O (≥99.9%), $C_2H_2O_4{\cdot}2H_2O$ (≥99.9%), $C_7H_6O_3$ (≥99.5%), $C_6H_5Na_3O_7$ (≥99.5%), LiF (≥99.9%), $LiClO_4$ (≥99.9%), HCl (37%) and Nafion (5 wt%) were obtained from Sinopharm Chemical Reagent Co., Ltd. $Na_2MoO_4{\cdot}2H_2O$ (≥99.5%), $C_4H_4O_6KNa{\cdot}4H_2O$ (≥99.9%), NaClO (≥99.9%), $C_9H_{11}NO$ (≥99.5%), $C_5FeN_6Na_2O$ (≥99.0%), $C_{12}H_{14}N_2{\cdot}2HCl$ (≥99.0%), N_2H_4 (≥99.9%), H_2SO_4 (98%), NH_4Cl (≥99.5%), $SO_2(NH_2)_2$ (≥99.5%), D_2O (≥99.9%) and DMSO (≥99.0%) were purchased from Sigma-Aldrich Chemical Reagent Co., Ltd.

Synthesis of TiS_2

TiS_2 was synthesized using a facile liquid exfoliation method. Initially, bulk TiS_2 powders were dissolved in isopropyl alcohol and the initial concentration was 7.5 mg/mL. The mixed solution was sonicated for 90 minutes and then the dispersions were allowed to stand for 24 h. Afterwards, the mixture was centrifuged at 1500 rpm for 2 h to collect the precipitate and dried to produce TiS_2.

Electrochemical experiment

Electrochemical measurements were conducted under ambient conditions on a CHI-760E electrochemical workstation. The graphite rod, Ag/AgCl, and CC-loaded catalyst served as the reference, counter, and working electrodes, respectively. All potentials were referenced to reversible hydrogen electrode (RHE) by E (V vs. RHE) = E (V vs. Ag/AgCl) + 0.198 V + 0.059 × pH. The electrocatalytic NORR measurements were conducted within a gas-tight H-cell, using NO-saturated 0.5 M Na_2SO_4 electrolyte. Before NRR testing, the feeding gases were purified using two glass bubblers filled with 4 M KOH solution[1]. Furthermore, the cathodic compartment was flushed with Ar for a minimum of 30 minutes to eliminate any remaining oxygen. Throughout the NRR electrolysis process, a continuous flow of NO (99.9%) gas was introduced into the cathodic chamber at a rate of 20 mL min^{-1}. Subsequent to an hour of electrolysis, both the aqueous and gaseous products were identified using colorimetric methods and gas chromatography (GC), respectively.

Determination of NH_3

The generated NH_3 was determined by the indophenol blue method[2]. Typically, 0.5 mL electrolyte was removed from the electrochemical reaction vessel and diluted 10 times with deionized water. Then 2 mL diluted solution was removed into a clean vessel followed by sequentially adding NaOH solution (2 mL, 1 M) containing $C_7H_6O_3$ (5 wt.%) and $C_6H_5Na_3O_7$ (5 wt.%), NaClO (1 mL, 0.05 M), and $C_5FeN_6Na_2O$ (0.2 mL, 1wt.%) aqueous solution. After the incubation for 2 h at room temperature, the mixed solution was subjected to UV-vis measurement using the absorbance at 655 nm wavelength. The concentration-absorbance curves were calibrated by the standard NH_4Cl solution with a series of concentrations, and the NH_3 yield rate and NH_3-Faradaic efficiency (FE_{NH3}) were calculated by the following equation[1]:

$$NH_3 \text{ yield rate} = (c \times V) / (17 \times t \times A) \quad (1)$$

NH_3-Faradaic efficiency (FE_{NH3}) was calculated by the following equation:

$$FE_{NH3} = (5 \times F \times c \times V) / (17 \times Q) \times 100\% \quad (2)$$

where c (μg mL^{-1}) is the measured NH_3 concentration, V (mL) is the volume of electrolyte in the cathode chamber, t (s) is the electrolysis time and A is the surface area of CC (1×1 cm^2), F (96500 C mol^{-1}) is the Faraday constant, Q (C) is the total quantity of applied electricity.

The detailed procedures for colorimetric determination of N_2H_4 was provided in our previous publication[3].

Characterizations

X-ray diffraction (XRD) was performed on a Rigaku D/max 2400 diffractometer. Transmission electron microscopy (TEM) and high-resolution transmission electron microscopy (HRTEM) were performed on a Tecnai G^2 F20 microscope. X-ray photoelectron spectroscopy (XPS) analysis was collected on a PHI 5702 spectrometer.

Calculation details

Spin-polarized density functional theory (DFT) calculations were carried out using the Cambridge sequential total energy package (CASTEP) with projector augmented wave pseudopotentials. The Perdew-Burke-Ernzerhof (PBE) generalized gradient approximation (GGA) functional was used for the exchange-correlation

potential. The van der Waals interaction was described by using the empirical correction in Grimme's scheme (DFT+D). During the geometry optimization, the electron wave functions were expanded using plane waves with a cutoff energy of 500 eV. The convergence tolerance was set to be 1.0×10^{-5} eV for energy and 0.02 eV $Å^{-1}$ for force. The 4 × 4 × 1 Monkhorst-Pack mesh was used in Brillouin zone sampling. TiS_2 (011) was modeled by a 4 × 4 supercell, and a vacuum region of 15 Å was used to separate adjacent slabs.

The adsorption energy (ΔE) is defined as[4]

$$\Delta E = E_{\text{ads/slab}} - E_{\text{ads}} - E_{\text{slab}} \quad (3)$$

where $E_{\text{ads/slab}}$, E_{ads} and E_{slab} are the total energies for adsorbed species on slab, adsorbed species and isolated slab, respectively.

The Gibbs free energy (ΔG, 298 K) of reaction steps is calculated by[4]

$$\Delta G = \Delta E + \Delta ZPE - T\Delta S \quad (4)$$

where ΔE is the adsorption energy, ΔZPE is the zero-point energy difference and $T\Delta S$ is the entropy difference between the gas phase and adsorbed state.

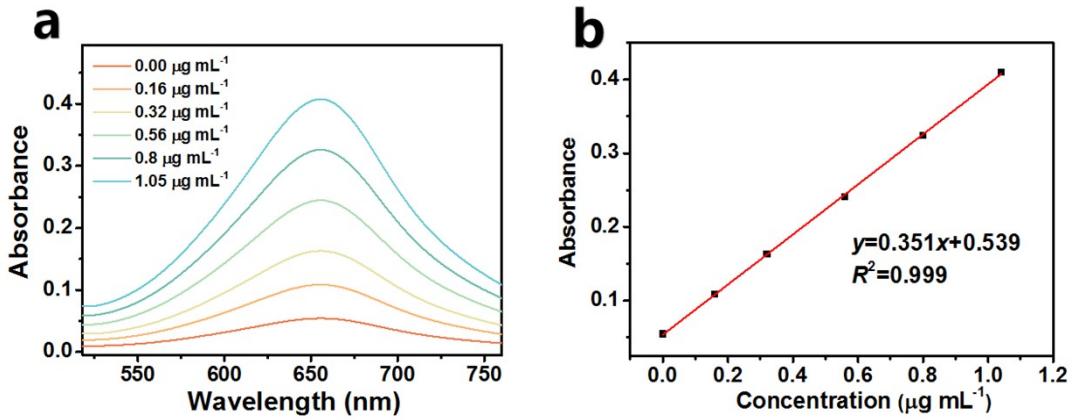

Fig. S1. (a) UV-vis absorption spectra of NH_4Cl assays after incubated for 2 h at ambient conditions. (b) Calibration curve used for the calculation of NH_3 concentrations.

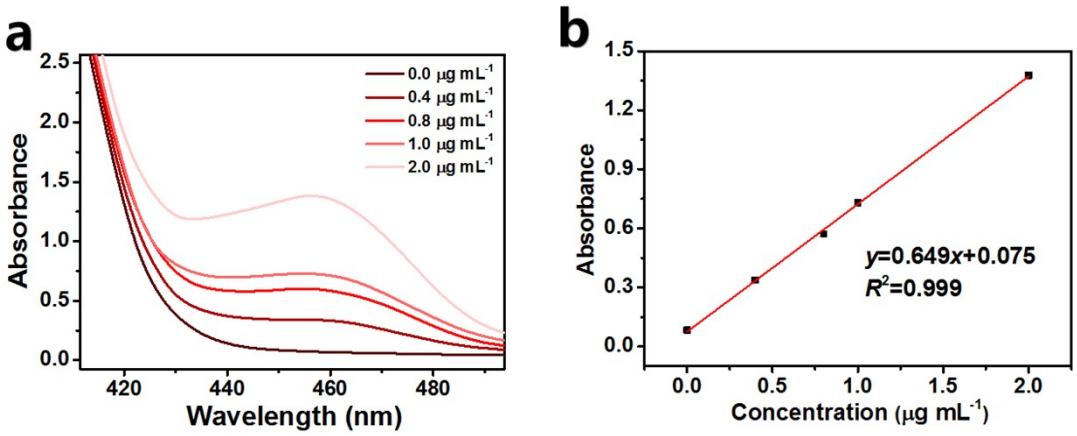

Fig. S2. (a) UV-vis absorption spectra of N_2H_4 assays after incubated for 20 min at ambient conditions. (b) Calibration curve used for calculation of N_2H_4 concentrations.

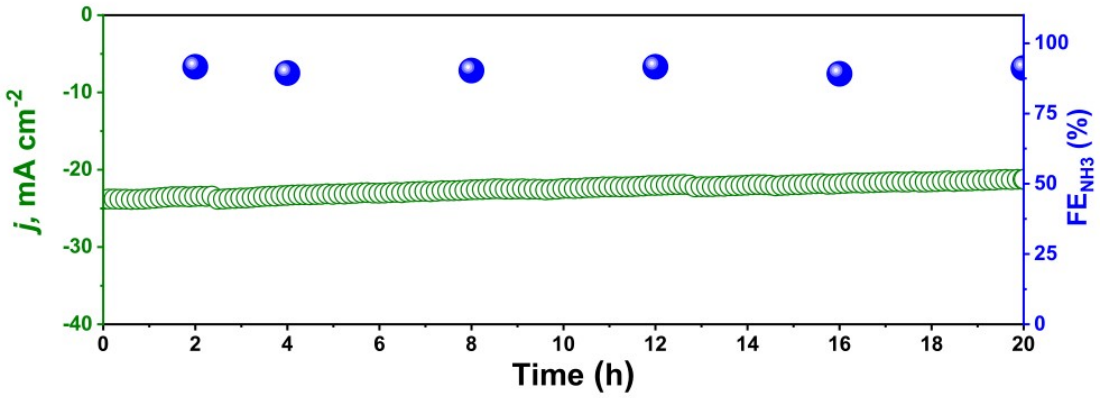

Fig. S3. Long-term chronoamperometry test of TiS_2 for 20 h at -0.6 V.

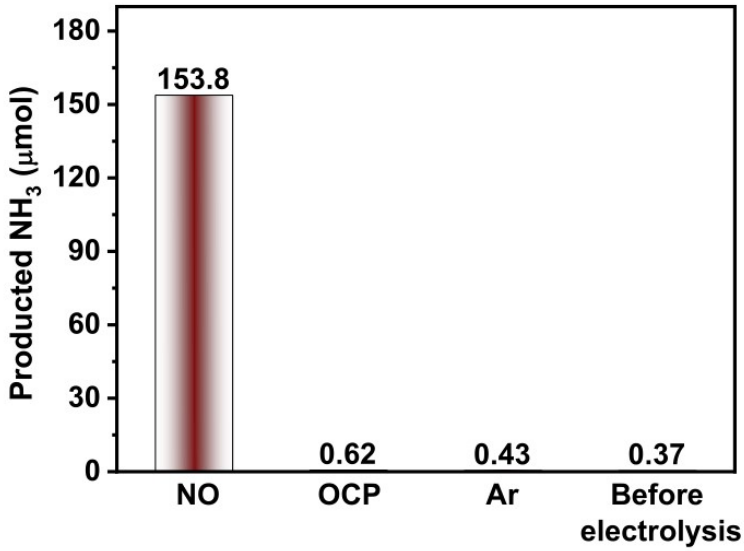

Fig. S4. Amounts of produced NH_3 over TiS_2 under different conditions at -0.6 V.

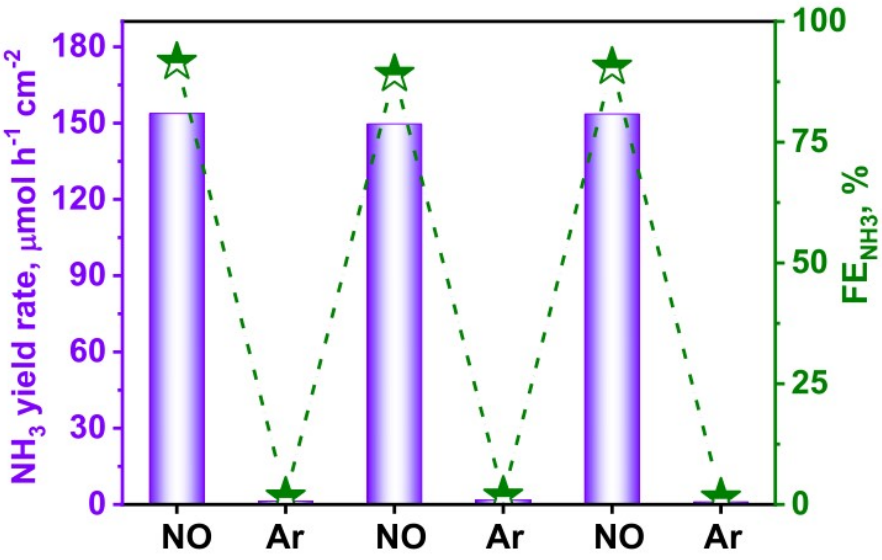

Fig. S5. NO-Ar gas switching experiment on TiS_2 at -0.6 V.

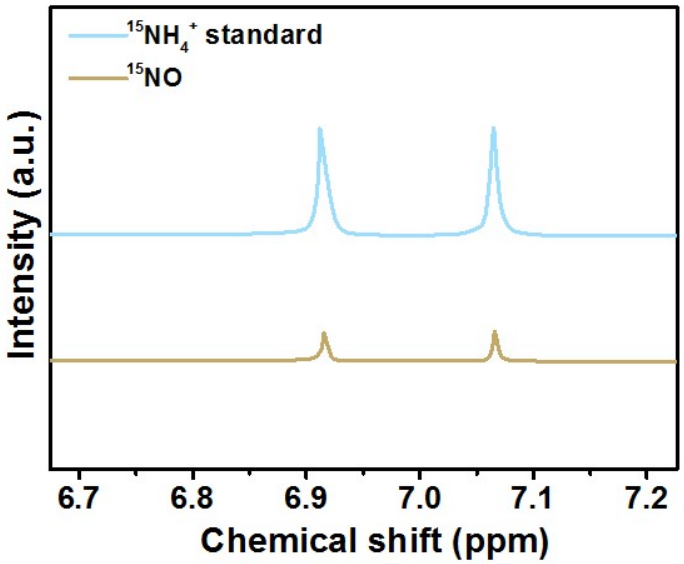

Fig. S6. ^{1}H NMR spectra of $^{15}NH_4^+$ standard sample and those fed by ^{15}NO after NORR electrolysis on TiS_2 at -0.6 V.

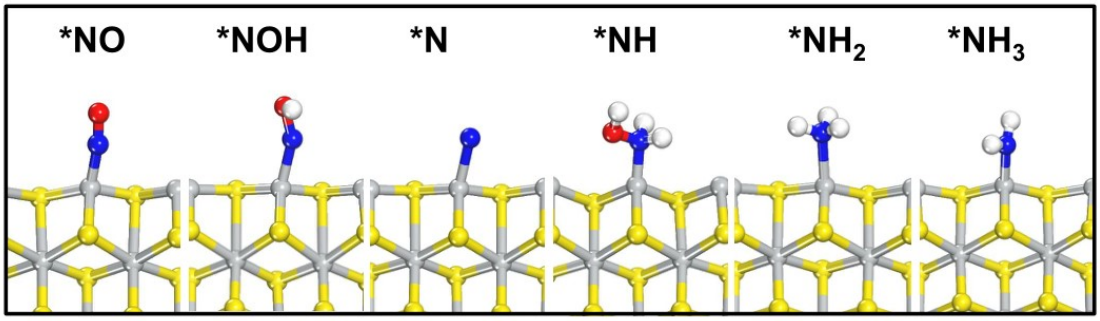

Fig. S7. Optimized structures of the reaction intermediates for NOH pathway on TiS_2.

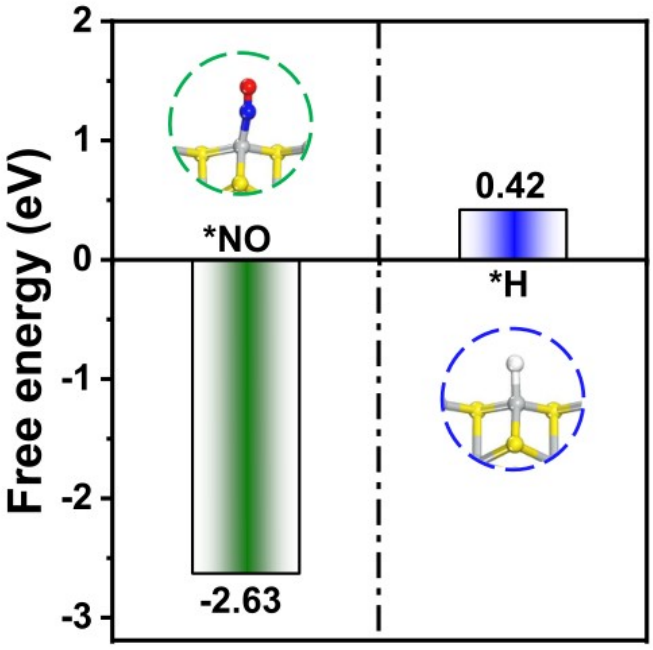

Fig. S8. Comparison of the *H/*NO binding free energies on TiS_2.

Table S1. Comparison of the optimum NH_3 yield rate and NH_3-Faradic efficiency (FE_{NH3}) for recently reported NORR electrocatalysts at ambient conditions.

Catalyst	Electrolyte	NH_3 yield rate ($\mu mol\ h^{-1}\ cm^{-2}$)	FE_{NH3}	Potential (V vs. RHE)	Ref.
FeP/CC	0.2 M PBS	85.62	88.49%	-0.2	[5]
NiO/TM	0.1 M Na_2SO_4	125.3	90%	-0.6	[6]
Ni_2P/CP	0.1 M HCl	33.47	76.9%	-0.2	[7]
a-$B_{2.6}C$@TiO_2 /Ti	0.1 M Na_2SO_4	216.4	87.6%	-0.9	[8]
$Ru_{0.05}Cu_{0.95}$	0.05 M Na_2SO_4	17.68	64.9%	-0.5	[9]
Bi NDs	0.1 M Na_2SO_4	70.2	89.2%	-0.5	[10]
MoC/NCS	0.1 M HCl	79.4	89%	-0.8	[11]
CoP/TM	0.2 M Na_2SO_4	47.22	88.3%	-0.2	[12]
MoS_2/GF	0.1 M HCl	99.6	76.6%	0.1	[1]
CoS_{1-x}	0.2 M Na_2SO_4	44.67	53.62%	-0.4	[13]
Mo_2C	0.5 M Na_2SO_4	122.7	86.3%	-0.4	[3]
HCNF	0.2 M Na_2SO_4	22.35	88.33%	-0.6	[14]
TiS_2	**0. 5 M Na_2SO_4**	**153.8**	**91.6%**	**-0.6**	**This work**

References

[1]. L. Zhang, J. Liang, Y. Wang, T. Mou, Y. Lin, L. Yue, T. Li, Q. Liu, Y. Luo, N. Li, B. Tang, Y. Liu, S. Gao, A. A. Alshehri, X. Guo, D. Ma and X. Sun, *Angew. Chem. Int. Edit.*, 2021, **60**, 25263-25268.

[2]. P. Li, Z. Jin, Z. Fang and G. Yu, *Energy Environ. Sci.*, 2021, **14**, 3522-3531.

[3]. K. Chen, P. Shen, N. Zhang, D. Ma and K. Chu, *Inorg. Chem.*, 2023, **62**, 653-658.

[4]. G. Zhang, Y. Wan, H. Zhao, Y.-L. Guo and K. Chu, *Dalton Trans.*, 2023, **52**, 6248-6253.

[5]. J. Liang, Q. Zhou, T. Mou, H. Chen, L. Yue, Y. Luo, Q. Liu, M. S. Hamdy, A. A. Alshehri, F. Gong and X. Sun, *Nano Res.*, 2022, **15**, 4008-4013.

[6]. P. Liu, J. Liang, J. Wang, L. Zhang, J. Li, L. Yue, Y. Ren, T. Li, Y. Luo, N. Li, B. Tang, Q. Liu, A. M. Asiri, Q. Kong and X. Sun, *Chem. Commun.*, 2021, **57**, 13562-13565.

[7]. T. Mou, J. Liang, Z. Ma, L. Zhang, Y. Lin, T. Li, Q. Liu, Y. Luo, Y. Liu, S. Gao, H. Zhao, A. M. Asiri, D. Ma and X. Sun, *J. Mater. Chem. A*, 2021, **9**, 24268-24275.

[8]. J. Liang, P. Liu, Q. Li, T. Li, L. Yue, Y. Luo, Q. Liu, N. Li, B. Tang, A. A. Alshehri, I. Shakir, P. O. Agboola, C. Sun and X. Sun, *Angew. Chem. Int. Ed.*, 2022, **61**, e202202087.

[9]. J. Shi, C. Wang, R. Yang, F. Chen, N. Meng, Y. Yu and B. Zhang, *Sci. China Chem.*, 2021, **64**, 1493-1497.

[10]. Y. Lin, J. Liang, H. Li, L. Zhang, T. Mou, T. Li, L. Yue, Y. Ji, Q. Liu, Y. Luo, N. Li, B. Tang, Q. Wu, M. S. Hamdy, D. Ma and X. Sun, *Mater. Today Phys.*, 2022, **22**, 100611.

[11]. G. Meng, M. Jin, T. Wei, Q. Liu, S. Zhang, X. Peng, J. Luo and X. Liu, *Nano Res.*, 2022, **15**, 8890-8896.

[12]. J. Liang, W.-F. Hu, B. Song, T. Mou, L. Zhang, Y. Luo, Q. Liu, A. A. Alshehri, M. S. Hamdy, L.-M. Yang and X. Sun, *Inorg. Chem. Front.*, 2022, **9**, 1366-1372.

[13]. L. Zhang, Q. Zhou, J. Liang, L. Yue, T. Li, Y. Luo, Q. Liu, N. Li, B. Tang, F. Gong, X. Guo and X. Sun, *Inorg. Chem.*, 2022, **61**, 8096-8102.

[14]. L. Ouyang, Q. Zhou, J. Liang, L. Zhang, L. Yue, Z. Li, J. Li, Y. Luo, Q. Liu, N. Li, B. Tang, A. Ali Alshehri, F. Gong and X. Sun, *J. Colloid Interface Sci.*, 2022, **616**, 261-267.